IRWIN AND JOAN JACOBS
CENTER FOR COMMUNICATION AND INFORMATION TECHNOLOGIES

Tight Focusing of Wavefronts with Piecewise Constant Phase

Alexander Normatov, Boris Spektor and Joseph Shamir

CCIT Report #681
January 2008

DEPARTMENT OF ELECTRICAL ENGINEERING
TECHNION - ISRAEL INSTITUTE OF TECHNOLOGY, HAIFA 32000, ISRAEL

CCIT Report #681 January 2008

Tight Focusing of Wavefronts with Piecewise Constant Phase

Alexander Normatov*, Boris Spektor and Joseph Shamir

Department of Electrical Engineering, Technion – Israel Institute of Technology; Technion City, Haifa 32000, Israel
**Corresponding author: alexn@tx.technion.ac.il*

Abstract: The Richards-Wolf approach to analyze tight focusing by high numerical aperture aplanatic optical systems can only be applied to incident waves having a planar (or negligibly curved) wavefront at the entrance pupil. In some cases, however, such as certain singular beams, the incident wave can be represented by a wavefront with, approximately, piecewise constant phase. For wavefronts of this kind we extend the validity of the Richards-Wolf approach to approximate evaluation of the field distribution in the vicinity of the geometrical focus. The proposed method is applied to the derivation of the focal distribution obtained by placing a mask with a π phase shift at the entrance pupil.

OCIS codes: (050.1755) Computational electromagnetic methods; (050.1960) Diffraction theory; (260.6042) Singular optics.

References and links

1. B. Richards and E. Wolf, "Electromagnetic diffraction in optical systems, II Structure of the image field in an optical system", *Proc. R. Soc. Lond. A.* **253**, 358-379 (1959).
2. A. Yoshida, T. Asakura, "Electromagnetic field near the focus of Gaussian beams", Optik **41**(3), 281-92 (1974)
3. R. Kant, "An analytical solution of vector diffraction for focusing optical systems", J. of Modern Optics **40**(2), 337-347 (1993).
4. P. Torok, P. Varga Z., Laczik and G. R. Booker, "Electromagnetic diffraction of light focused through a planar interface between materials of mismatched refractive indices: an integral representation", J. Opt. Soc. Am. A. **12**(2), 325-332 (1995).
5. P. Torok, P. Varga and G. R. Booker, "Electromagnetic diffraction of light focused through a planar interface between materials of mismatched refractive indices: structure of the electromagnetic field", J. Opt. Soc. Am. A. **12**(10), 2136-2144 (1995).
6. P. Torok, P. Varga and G. Nemeth, "Analytical solution of the diffraction integrals and interpretation of wave-front distortion when light is focused through a planar interface between materials of mismatched refractive indices", J. Opt. Soc. Am. A. **12**(12), 2660-2671 (1995).
7. C. J. R. Sheppard and P. Torok, "Efficient calculation of electromagnetic diffraction in optical systems using a multipole expansion", J. of Modern Optics **44**(4), 803-818 (1997).
8. K. S. Youngworth and T. G. Brown, "Focusing of high numerical aperture cylindrical vector beams", Opt. Ex. **7**(2), 77-87 (2000).
9. C. J. R. Sheppard, "High-aperture beams", J. Opt. Soc. Am. A. **18**(7), 1579-1587 (2001).
10. P. Torok and P.R.T. Munro, "The use of Gauss-Laguerre vector beams in STED microscopy", Opt. Ex. **12**(5), 3605-3617 (2004).
11. S. S. Sherif and P. Torok, "Eigenfunction representation of the integrals of the Debye–Wolf diffraction formula", J. of Modern Optics **6**(15), 857-876 (2005).
12. Gilad M. Lerman and Uriel Levy, "Tight focusing of spatially variant vector optical fields with elliptical symmetry of linear polarization", Opt. Lett. **32**(15), 2194-2196 (2007).
13. B. Spektor, A. Normatov, and J. Shamir, "Singular beam microscopy," Appl. Opt. **47**, A78-A87 (to be published in 2008).
14. Y. Li and E. Wolf, "Three-dimensional intensity distribution near the focus in systems of different Fresnel numbers", J. Opt. Soc. Am. A **1**(8), 801-808 (1984).
15. B. Spektor R. Piestun, and J. Shamir, "Dark Beams with a constant notch", Opt. Letters **21**, 456-458 (1996).
16. J. Shamir, *Optical Systems and Processes* (SPIE, 1999).

17. S. Quabis, R. Dorn, M. Eberler, O. Glockl, G. Leuchs, "The focus of light – theoretical calculation and experimental tomographic reconstruction", Appl. Phys. B **72**, 109–113 (2001).

1. Introduction

Recent advances in nanotechnology and nanofabrication drive the need for tighter focusing of light, requiring high numerical aperture (NA) optical systems. A popular approach for analyzing high NA aplanatic focusing systems with rotational symmetry was pioneered by Richards and Wolf in 1959 [1]. They derived expressions for an optical field in the vicinity of the geometric focus for the case of uniformly polarized incident plane wave illumination at the entrance pupil. Afterwards, corresponding expressions were derived for Gaussian beam amplitude distribution at the entrance pupil [2] and later the Seidel aberrations at the exit pupil of the focusing optical system [3] were considered. An important aspect of focusing through planar interface between materials of mismatched refractive indices was addressed in Refs. [4-6]. A generalization for radially symmetric, infinite Fresnel number systems was introduced with help of multipole extension [7]. Integral expressions for the specific cases of radially and azimuthally polarized tightly focused beams, having a planar phase at the entrance pupil were derived in Ref. [8] while a fundamental discussion and classification of high numerical aperture beams was performed in Ref. [9]. Analysis of focusing of Gauss-Laguerre vector beams [10, 11] required the inclusion of azimuthally changing phase. Although it was admitted that a varying phase of the incident illumination invalidated the basic assumption of Richards-Wolf (RW) approach, it was justified on condition that the phase variation was slow, and thus the solution could still be approximated with expressions corresponding to a planar wavefront.

The different variants and modifications of the RW approach mentioned above made use of symmetry of the investigated problem or the analytical properties of the function, describing the illumination incident on the entrance pupil, in order to reduce the computational complexity. This complexity reduction was achieved by analytical derivation of the azimuthal integration, thus leaving only the polar integration to numerical evaluation. Recent advances in computing capabilities have allowed direct numerical evaluation of the double integration (both azimuthal and polar). This allowed analyzing problems where the azimuthal integration could not be performed analytically [12].

The present work was motivated by the need to derive the focal distribution for a mask containing a π phase shift. The wavefront generated by this mask belongs to a class of wavefronts that can be approximately represented by piecewise constant phase segments, where the boundary region between neighboring constant-phase segments is relatively narrow but their relative phases are arbitrary. Each such segment alone lends itself to a treatment by the RW approach and this is exploited here to derive the focal distribution of an aplanatic optical system when this wavefront is incident on its entrance pupil. As we do not limit the applicability of the suggested method to symmetrically (or otherwise) reducible problems we perform the direct numerical integration both along the azimuthal as well as the polar angles. Obviously, for specific problems an analytic reduction of the integration remains still possible. The theoretical outline of the proposed method is introduced in the next section and a case study is performed in Sect. 3 to derive the focal field structure of a singular beam for high and medium NA optical systems. Beams of this kind are utilized for the recently introduced procedure of singular beam microscopy [13]. Section 4 evaluates the influence of our approximations on the resulting accuracy and then conclusions are drawn.

2. Theory

The RW method [1] requires that the incident optical wave at the entrance pupil of a focusing aplanatic optical system is adequately represented by rays parallel to the optical axis. This requirement, however, contradicts phase variations in the plane of the entrance pupil. As indicated above, our interest here is in optical wavefronts that can be segmented in such a way

that each segment by itself can be handled by the RW method. Accordingly we assume that the wavefront incident on the aperture has, to a good degree of approximation, a piecewise constant phase, thus comprising a finite set of almost constant-phase segments. In addition, we assume that only a small fraction of the energy in the incident field is contained in regions where non-negligible phase variations occur, in particular in the boundaries between neighboring segments. Under these conditions it is possible to use the principle of superposition to evaluate the field in the focal region as a linear superposition of the contributions obtained from each constant-phase segment of the incident field. It should be noted that no assumptions are made about the incident optical field amplitude or polarization.

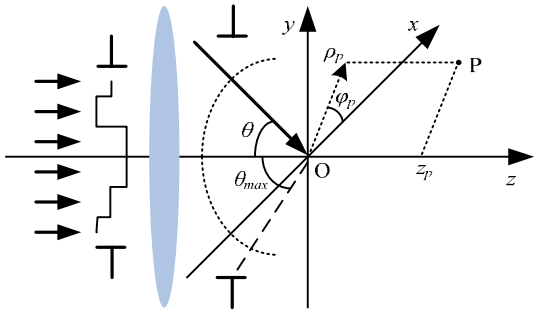

Fig. 1. Schematic illustration of the investigated problem.

With the above assumptions, the summation of contributions of rays associated with the different constant-phase segments of the incident wavefront is accomplished by integrals derived in a similar way as described in Refs. [1] and [8]:

$$\begin{aligned}\bar{E}\left(\rho_P,\varphi_P,z_P\right) = -\frac{if}{\lambda}\int_0^{\theta_{\max}}\int_0^{2\pi}\left\{l_0^x\left(\varphi,\theta\right)\exp\left[i\gamma_0^x\left(\varphi,\theta\right)\right]\bar{M}\right\}d\varphi d\theta - \\ -\frac{if}{\lambda}\int_0^{\theta_{\max}}\int_0^{2\pi}\left\{l_0^y\left(\varphi,\theta\right)\exp\left[i\gamma_0^y\left(\varphi,\theta\right)\right]\bar{N}\right\}d\varphi d\theta\end{aligned} \tag{1}$$

where:

$$\bar{M} = V\times\begin{pmatrix}\cos\theta+\sin^2\varphi\left(1-\cos\theta\right)\\ \sin\varphi\cos\varphi\left(\cos\theta-1\right)\\ \sin\theta\cos\varphi\end{pmatrix}\quad \bar{N} = V\times\begin{pmatrix}\cos\varphi\sin\varphi\left(\cos\theta-1\right)\\ 1-\sin^2\varphi\left(1-\cos\theta\right)\\ \sin\theta\sin\varphi\end{pmatrix} \tag{2}$$

$$\begin{aligned}V = \exp\left\{ik\left[-\left(\sin\theta\cos\varphi\right)\rho_P\cos\varphi_P-\left(\sin\theta\sin\varphi\right)\rho_P\sin\varphi_P+\left(\cos\theta\right)Z_P\right]\right\}\times \\ \times\sin\theta\sqrt{\cos\theta}\end{aligned} \tag{3}$$

In Eq. (1) $\bar{E}\left(\rho_P,\varphi_P,z_P\right)$ represents the electric field at a point $\mathrm{P}\left(\rho_P,\varphi_P,z_P\right)$ located in the vicinity of the geometrical focus, O, of the optical system, as shown in Fig. 1. The focal distance of the system is f and its NA defines the maximum half aperture angle, $\theta_{\max}=\sin^{-1}(NA)$. The wavelength, λ, determines the propagation constant, $k=2\pi/\lambda$. The angle θ is defined between the negative direction of the z axis and the negative direction

of a ray emerging from the exit pupil and directed toward O. The origin of the Cartesian coordinate system, *x,y,z,* and of the cylindrical coordinate system, ρ, φ, z, are located at the geometrical focal point, O. The azimuthal angle, φ, of a projection of an emerging ray onto the *xy* plane, is defined between the projection and the positive direction of the *x* axis and the projection radius is $\rho = \left(x^2 + y^2\right)^{1/2}$. The *x* and *y* polarization components of the incident optical field are described by their corresponding amplitudes (similar to Ref. [1]), $l_0^x(\varphi,\theta)$ and $l_0^y(\varphi,\theta)$ and phases, $\gamma_0^x(\varphi,\theta)$ and $\gamma_0^y(\varphi,\theta)$. It must be noted that although the mathematical notation allows for an arbitrary amplitude, phase and polarization of the incident transversal field, the phase variation and actual summation is still subject to the conditions stated above. Following the same assumptions, the *z* component of the incident optical field is neglected.

As we do not make any assumptions about the geometrical shapes of the various segments (outlined by non-negligible phase variations), the coordinates are not separable. This implies that in a general case the analysis must be implemented by a full, two-dimensional numerical evaluation.

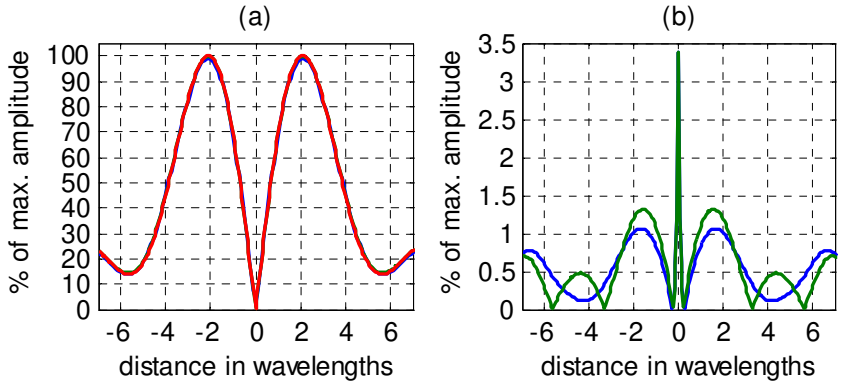

Fig. 2. Comparison of amplitude cross sections along the *x*-axis at the focal plane, for a π phase mask at the entrance pupil. Normalized amplitude values (a): paraxial scalar calculation – blue, rigorous calculation by the suggested method for *x* polarized incident illumination – green, *y* polarized incident illumination – red. (b) Normalized amplitude differences between the paraxial scalar result and rigorous results corresponding to *x* polarized incident illumination – blue, and *y* polarized incident illumination – green.

3. Focal field structure

The proposed procedure enables the approximate numerical evaluation of tight focusing of an incident optical field having approximately piecewise constant phase with arbitrary amplitude and polarization. To estimate the level of accuracy, the results derived by the present approach, must be compared to results obtained by a method which is not based on the RW approach, since Eq. (1) becomes the original RW expression by setting $\gamma_0^x(\varphi,\theta)$ and $\gamma_0^y(\varphi,\theta)$ equal zero. Consequently, an interesting comparison can be performed with a paraxial scalar calculation in a domain where it is applicable, such as for a medium numerical apertures, like NA=0.2. This numerical aperture corresponds to a half aperture angle of roughly 12 degrees, well within the domain suitable for paraxial scalar approximation. For the visible range and a standard microscope objective, the Fresnel number for this NA is about 500, which also makes it suitable for rigorous focusing analysis [14]. As a test case we chose a Dark Beam [15], which motivated this work.

The Dark Beam can be generated by a uniformly polarized plane wave passing through a phase mask containing a line phase dislocation. In our case we use a phase mask with an amplitude transmittance function $T(x,y)=\mathrm{sign}(x)$. When used in a rotationally symmetric optical system, this mask defines two half circles connected along the *y* axis. We consider the two polarization states along the *x* and the *y* axes. Numerical evaluation results are presented in Fig. 2, which shows a comparison of the cross sections along the *x* axis of the normalized amplitude at the focal plane. The difference between the scalar calculation (using paraxial operator approach [16]) and the proposed vector calculation is barely visible on the scale of the complete amplitude distribution (Fig. 2a). The difference can be observed only on an extended scale (Fig. 2b) where the difference is shown between the scalar result and the rigorous results corresponding to *x* and *y* incident polarizations. As indicated by Fig. 2b, the discrepancy is of the order of 1.5% of the maximum amplitude. Part of this discrepancy, in particular the central peak, is due to discretization.

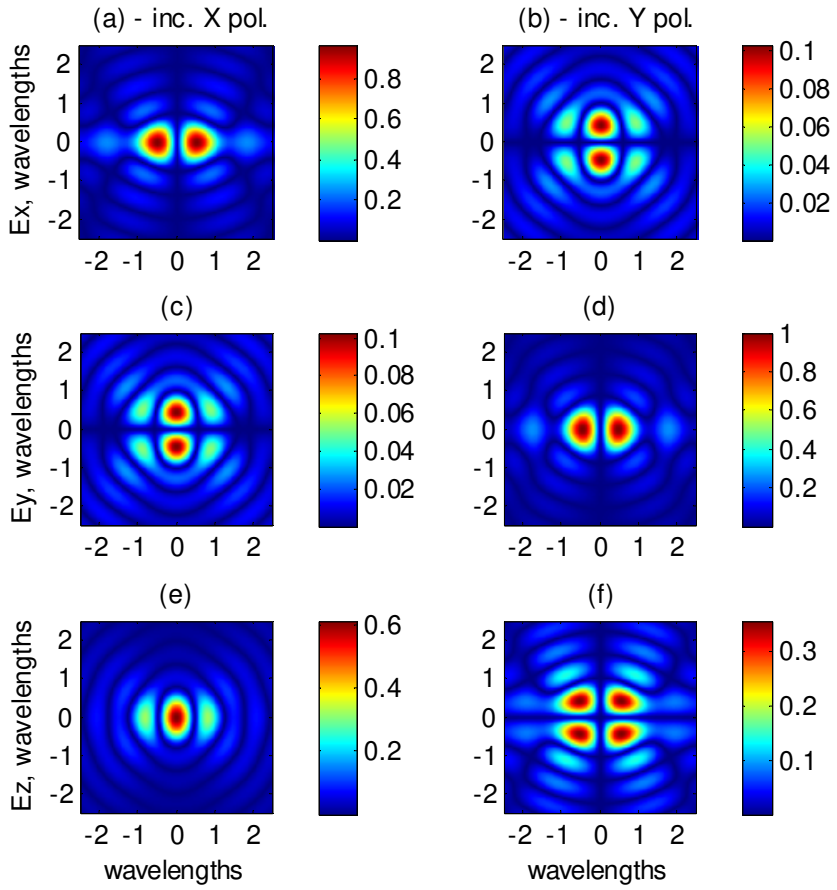

Fig. 3. Electric field components at the focal plane (*xy*) of an objective with NA=0.87, with a π half circle phase mask. For *x* polarized incident illumination (a), (c), (e) and *y* polarized incident illumination (b), (d), (f). Shown electric field components along *x* on (a), (b); along *y* on (c), (d); along *z* on (e), (f).

Applied to a high NA (NA=0.87) focusing of a Dark Beam, the present method generated the focal plane distributions of the electric fields components as shown in Fig. 3 for two

incident polarizations. The corresponding focal field optical intensity, which is proportional to $\left|\bar{E}\right|^2/2$ and the time averaged Poynting vector $\mathrm{Re}\left\{\bar{S}\right\}=\mathrm{Re}\left\{\bar{E}\times\bar{H}^*\right\}/2$ are shown in Fig. 4. Interestingly, the values of the time averaged Poynting vector are identical for the *x* and *y* polarization cases. An obvious reason is the duality in calculating the electric and magnetic fields (for *x* polarized electric field, the magnetic field is *y* polarized and vice versa). It is worth noting, at this point, that for the case of a plane wave incident illumination (without any phase mask) the distribution of the time averaged Poynting vector is circularly symmetric [1], while the corresponding electric field intensity has elliptical distribution [17]. Further discussion of the results and differences between the intensity distributions corresponding to the various polarizations is outside the scope of this paper.

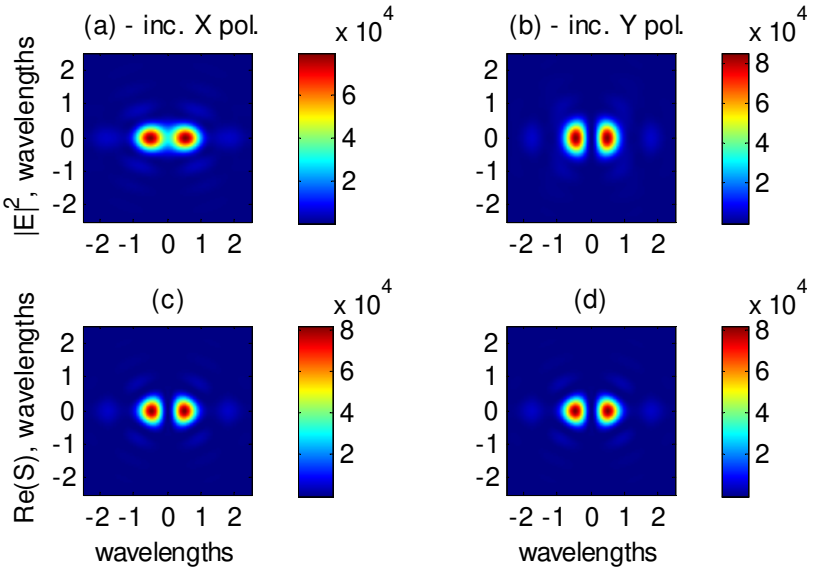

Fig. 4. Optical intensity (a), (b) (proportional to $|E|^2$) and time averaged Poynting vector (c), (d) corresponding to the fields of Fig. 3. For *x* polarized incident illumination (a), (c) and *y* polarized incident illumination (b), (d).

4. Influence of the segment boundaries

Up to this point we ignored possible influence of the boundaries between the various constant-phase segments. It is, however, important to assess the effects of finite (rather than infinitesimal) boundary width on the resulting accuracy. Since numerical evaluation implies a discretization of the incident optical field the smallest, non-zero boundary width is limited by the discretization parameters. In practice, this width will be determined by the phase mask fabrication process or by the characteristics of a spatial light modulator. Here we again use the Dark Beam example (with NA=0.87) and perform numerical evaluation for different relative orientations between the boundary and polarization direction. As a parameter for the analysis we consider the relative area occupied by the boundaries rather than just the boundary width. As discussed in Section 2, the contribution of incident rays that are associated with the boundary area is neglected. The total optical intensity distribution root mean square (RMS) error (related to intensity distribution corresponding to zero width boundary case and normalized by the maximum intensity of that distribution) is shown as a function of the boundary area in Fig. 5 for *x* (blue line) and *y* (green line) polarized incident illumination (the line phase dislocation on the phase mask is aligned along the *y* axis in both cases). The RMS error was evaluated over the area of the focal plane that is shown in Figs. 3, and 4. The results presented in Fig. 5 indicate that the RMS error is limited to about 0.05% for reasonable

boundary area (<2%), which is much less than the 2% power discarded at the boundaries. The flattening of the RMS error for low values of boundary area is probably due to the discretization that was kept constant regardless of the boundary width. A discussion of errors due to discretization is outside of the scope of this paper. It is interesting to note that in all the cases investigated the power evaluated over a larger area of the focal plane corresponds to the transmitted power of the incident illumination (thus energy conservation holds). Although the considered example included incident field polarizations that are either parallel (*y* polarized) or normal (*x* polarized) to the boundary, care should be taken when applying the results presented above to other incident optical field distributions.

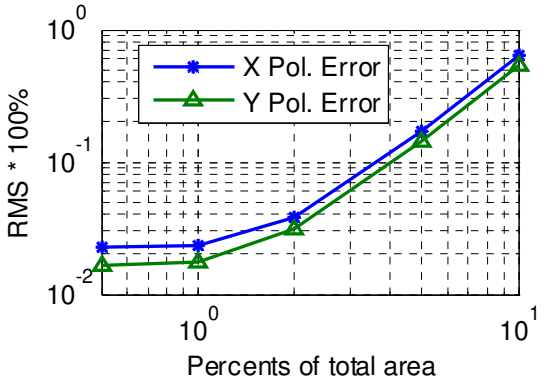

Fig. 5. Root mean square error related to maximum intensity as a function of boundary associated area.

5. Conclusion

We have shown that the applicability of the Richards-Wolf approach is extendable to handle optical fields that can be represented by wavefronts with, approximately, piecewise constant phase at the entrance pupil of an aplanatic focusing optical system. A numerical analysis for a specific case indicated that the method yields a good approximation. In particular, calculations performed for a focusing system that satisfies the paraxial approximation yielded results almost identical to a scalar calculation.

The suggested method provides a valuable degree of freedom in shaping the focal distribution in high NA optical systems. Thus, both scientific and technological applications using high NA optics can benefit from the new approximate numerical evaluation method. As a case study, the focal distribution of an optical beam, containing a phase singularity, was investigated. Such a beam is the key constituent in various procedures, such as singular beam microscopy. The technological applications range from nano-metrology, such as nano-positioning or nanoscale object evaluation, to optical storage devices.

Acknowledgments

This work was performed within the NANOPRIM project supported by the European Community under the FP6 program. BS thanks the Israel Ministry of Absorption for support provided to new-immigrant scientists. The authors are pleased to thank P. Török for reading the manuscript and providing constructive comments.